JOJ Material Science (JOJMS)

Juniper Publishers key to the Researchers

Research Article
Volume 4 Issue 2 - April 2018
DOI: 10.19080/JOJMS.2018.04.555635

JOJ Mater Sci

Time Dependent Microstructural and Magnetic Properties of Nanocrystalline $Fe_{67.6}Co_{16.9}Nb_5B_{8.5}P_2$ Metallic Alloy

K Gehlot[1], S S Modak[2], L K Varga[3] and S N Kane[1]*

[1]*Magnetic Materials Laboratory, School of Physics, D A University, Khandwa Road Campus, Indore, India*

[2]*Physics Department, Jaypee University of Eng & Tech, AB Road, Raghogarh, Guna, India*

[3]*RISSPO, Hungarian Academy of Sciences, 1525 Budapest, Hungary, India*

Submitted: March 21, 2018; **Published:** April 04, 2018

***Corresponding author:** Kane SN, Magnetic Materials Laboratory, School of Physics, D A University, Khandwa Road Campus, Indore, Email: kane_sn@yahoo.com

Abstract

Effect of thermal treatment on structural, magnetic properties of $Fe_{67.6}Co_{16.9}Nb_5B_{8.5}P_2$ partly nanocrystalline alloy has been studied via X-ray diffraction and magnetic measurements. XRD results show that after isothermal annealing treatment at 450°C the grain size range between 11.0 to 25.0 nm, and saturates to 24.5 nm. For the studied samples, the obtained lattice parameter shows the presence of pure bcc-Fe phase (without any presence of Co) which precipitates out from amorphous matrix. Coercivity and saturation magnetization values range respectively between 50 to 83 A/m and 1.8 to 1.5 Tesla. Time evolution of magnetic properties very clearly shows the correlation with structural changes.

Keywords : Metallic glass; Nanostructured grains; X-ray diffraction; Magnetic properties

Introduction

Fe-based bulk metallic glasses possess good glass forming ability, high thermal stability, high strength and excellent soft magnetic behavior [1]. The combination of nano grain size and good soft magnetic properties have many applications [2]. Vital studies e.g. [3,4] concluded that Fe based amorphous alloys appear to improve the saturation magnetization and having low losses, needed for industrial applications. Si free nanoperm alloy displays good soft magnetic properties, and the presence of Co improves Curie temperature of amorphous matrix and precipitating crystalline phase [5]. Fe-Co containing alloys exhibit high saturation magnetization (1.8 T), so the amount of Nb and B needs to be reduced in the alloy. It may be noted that the absence of Zr in the alloys helps them to be casted in air. P addition is very effective in widening the optimum annealing temperature range and refining of bcc-Fe grains size in addition to increasing of nano crystalline grains density [6]. Thermal treatment near crystallization temperature is known to relax the material structurally, thus affecting the microstructure. Therefore, in the present work we report the effect of isothermal annealing on time evolution of structural and magnetic properties of $Fe_{67.6}Co_{16.9}Nb_5B_{8.5}P_2$ alloy.

Experiments

Amorphous alloy ribbons of nominal composition $Fe_{67.6}Co_{16.9}Nb_5B_{8.5}P_2$ (4 mm wide, 20 μm thick) were prepared by planner flow casting method on a rotating copper wheel. Thermal treatments (between 15 minute to 60 minute at 450°C in an interval of 15 min) were performed in an inert (Ar) atmosphere. X-ray diffraction measurements were done using Brukar D8 Advance X-Ray Diffractometer with Cu-K_α radiation (λ =0.15406 nm) at UGC-DAE-CSR Indore. X-Ray Diffraction data was analyzed with the help of a MATLAB based program that fits the amorphous and crystalline components with pseudo voigt line profile described elsewhere [3]. Using the width of the (110) peak in Scherer's formula average grain diameter D was obtained. Lattice parameter a is calculated using Nelson-Taylor-Sinclair correction in order to take into account the peak shift due to sample offset. Hysteresis loops of as-cast and isothermally annealed specimens were carried out by the conventional induction hysteresis loop tracer at 50 Hz with a maximum applied field: i) ±3000 A/m to obtain saturated magnetization (M_s) values, and ii) ±1000 A/m to get coercivity (H_c).

Results and Discussions

Figure 1 depicts the XRD patterns of isothermally annealed samples annealed at 450˚C for different time, exhibiting structural evolution with time. Perusal of Figure 1 clearly shows that the as cast sample consists of overlapping of two peaks: one corresponds to amorphous matrix (broad amorphous hump), and the second one is the precipitated crystalline phased (sharp peak). As we increase the annealing time, broad hump gradually disappears and crystalline peaks start to appear with prominence suggesting the higher volume fraction of the crystalline phase. The primary crystallization stage creates bcc Fe nanocrystals, dispersed in residual amorphous matrix [7]. The relative intensities match well with the JCPDS database [8]. Choosing different annealing time would lead to various level of structural relaxation, and as a sequence specimen will become more ordered at higher annealing time. Also the presence of Phosphorus forms high density primary nucleation sites and facilitates the precipitation of Fe-Co type crystalline phase [9]. For the duration of annealing at time up to 60 min, no additional crystalline phase develops, as the peak remains at the same 2θ position. Lattice parameter for the studied as-cast sample is 0.2871 nm, which increases slightly (0.2877 nm) after 15 min. annealing, is ascribable to the presence of Nb (ionic radius of Fe = 156 pm and Nb = 198 pm) in the crystalline phase. Obtained lattice parameter clearly shows that Co is nearly absent in the precipitating bcc Fe. Grain diameter, and volume fraction of nanograins is calculated from XRD data. Figure 2 shows the evolution of grain size (D) and volume fraction (V_x) of nano grains as a function of annealing temperature, at different annealing time. It can be interpreted that after first isothermal treatment, due to the diffusion of Nb, grain diameter and volume fraction of nanograins increases respectively from 11 nm and 12% (observed for as quenched samples), and saturates ~ 24 nm, 74% for all the samples annealed for higher annealing times (within error bar practically remains same), as was also observed earlier [10]. Effect of isothermal annealing on hysteresis loops of the studied alloy, annealed for 15 min, 30 min, 45 min and 60 min, are represented in Figure 3, and its inset shows inflated coercivity. Magnetic parameters obtained by magnetic measurements are represented in table (inset of Figure 4). After annealing, marginal change were observed in the value of remanance (B_r) and the squareness ratio (B_r/B_s) as also reflected in B-H loops. For all annealed specimens, where crystallization process occurs, H_c shows considerable increase (shown in the inset of Figure 4), ascribable to increase in anisotropy due to grain growth [2,11,12]. As here H_c does not follow Random Anisotropy Model (as H_c increases, instead of its reduction), it can be accounted to domain wall pinning on the bcc-Fe nanograins due to local demagnetizing field. Further, increase of H_c after first heat treatment can be associated to the stress-relaxation, whereas further increase of H_c for the samples annealed for 60 min. is ascribable to domain wall pinning by growing nanostructured grains. Figure 4 depicts the H_c dependence of V_xD, while straight line shows linear fit to the data. Perusal of Figure 4 clearly follows the domain wall pinning theory described by Bertotti et al. [11]. According to two dimensional wall bowing [12], an explanation was provided on linear relationship between H_c and V_xD ($H_c \propto V_xD$) [11], as is also observed in the present work.

Figure 5 depicts the annealing time dependence of lattice parameter, whereas inset shows annealing time dependence of B_s. Perusal of Figure 5 (inset) shows that, as we move on from as-cast to annealed samples (for different times), a noticeable deterioration in M_s was observed. It should be noted that in sample annealed at 450˚C/15 min, an increase of lattice parameter with concurrent decrease of M_s is observed (see Figure 5 and its Inset). This observation indicates the presence of non-magnetic element 'Nb' (which has higher ionic radius than Fe) in the first near-neighbour shell of Fe present in the growing bcc-Fe, thus reducing the magnetic moment of Fe, reflected in the reduction of M_s. For higher annealing times, lowering of lattice parameter results in corresponding increase of M_s, indicating the presence of different Nb atoms in the growing bcc Fe-nano grains.

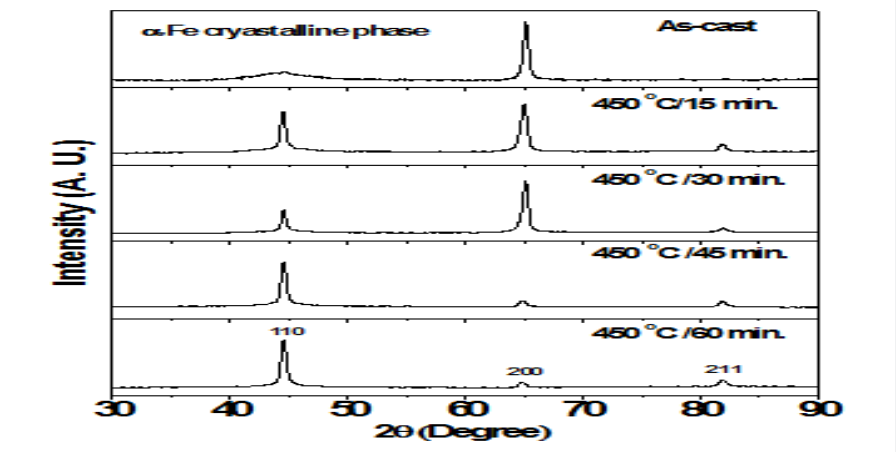

Figure 1: XRD patterns of as-cast and isothermally annealed samples at 450˚C.

How to cite this article: K Gehlot,S S Modak,L K Varga,S N Kane.Time Dependent Microstructural and Magnetic Properties of Nanocrystalline $Fe_{67.6}Co_{16.9}Nb_5B_{8.5}P_2$ Metallic Alloy. JOJ Mater Sci. 2018; 4(2): 555635. DOI: 10.19080/JOJMS.2018.04.555635

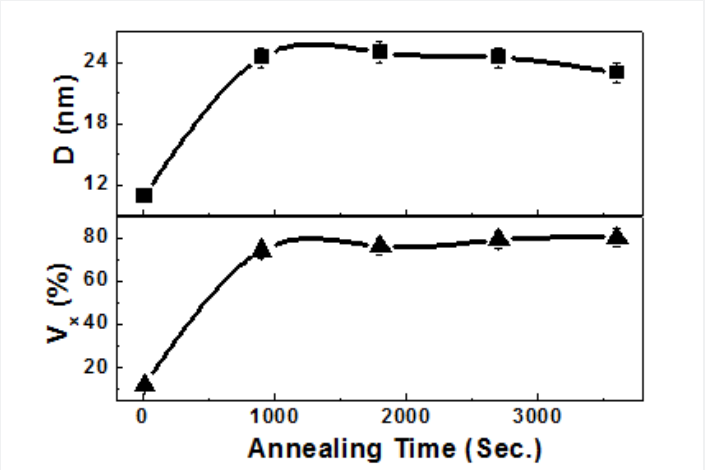

Figure 2: Annealing time dependent variation of grain size and volume fraction of nanograins.

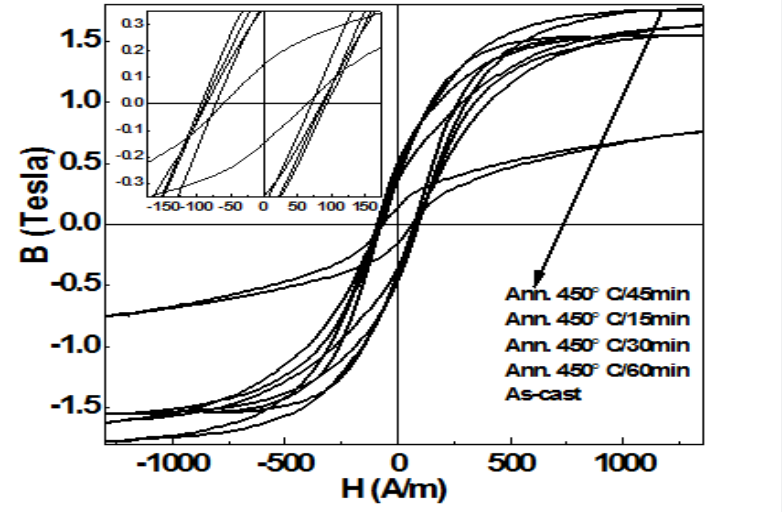

Figure 3: Hysteresis loops obtained at 50 Hz by Induction technique..

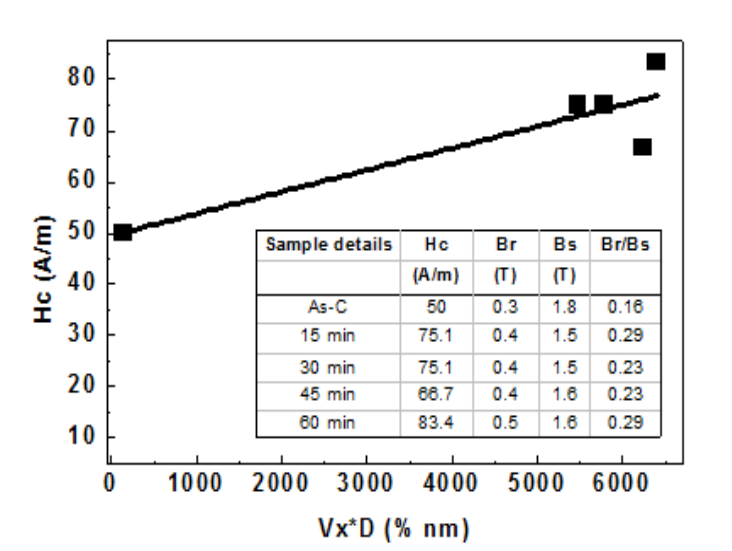

Sample details	Hc (A/m)	Br (T)	Bs (T)	Br/Bs
As-C	50	0.3	1.8	0.16
15 min	75.1	0.4	1.5	0.29
30 min	75.1	0.4	1.5	0.23
45 min	66.7	0.4	1.6	0.23
60 min	83.4	0.5	1.6	0.29

Figure 4: Linear graphic representing the correlation between H_c and V_xD.

How to cite this article: K Gehlot,S S Modak,L K Varga,S N Kane.Time Dependent Microstructural and Magnetic Properties of Nanocrystalline $Fe_{67.6}Co_{16.9}Nb_5B_{8.5}P_2$ Metallic Alloy. JOJ Mater Sci. 2018; 4(2): 555635. DOI: 10.19080/JOJMS.2018.04.555635

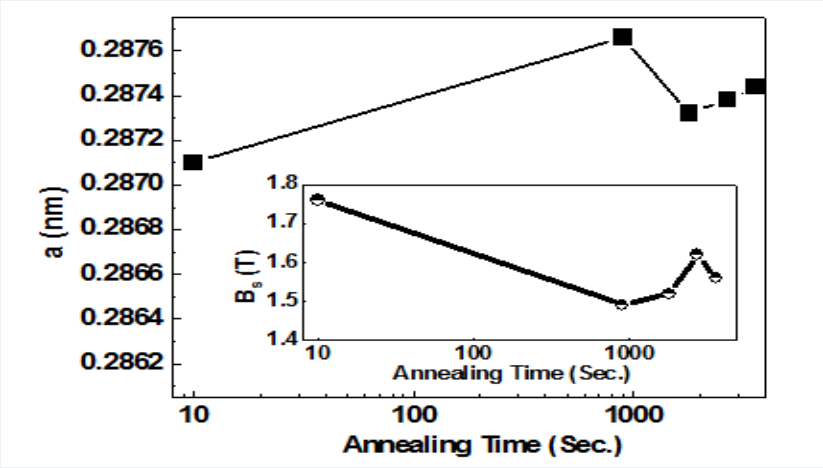

Figure 5: Effect of isothermal annealing on lattice parameter and magnetic induction.

Conclusion

X-ray diffraction, magnetic measurements were used to monitor the time evolution of structural and magnetic properties of $Fe_{67.6}Co_{16.9}Nb_5B_{8.5}P_2$ alloy, isothermally annealed at 450˚C for different times between 15 - 60 minutes. Isothermal treatment shows:

i) Formation of bcc Fe nanosrystalline phase with lattice parameter ranging between 0.2871-0.2877 nm.

ii) That with increasing annealing time both D and V_x are saturated.

iii) Presence of Nb in the growing nanocrystalline phase (grain diameter ranging between 11-25 nm), leading to concurrent increase of lattice parameter with decrease of saturation magnetization.

iv) Coercivity does not follow Random Anisotropy Model (as H_c increases, instead of its reduction), due to pinning of domain wall in growing bcc-Fe nanograins over 20 nm.

v) Linear dependence of H_c with V_xD further clarifies the applicability of domain wall pinning theory described by Bertotti [11] (instead of Random Anisotropy Model) in the studied specimens.

Acknowledgement

SNK is grateful for support in the framework of India-Portugal project No. IND/Portugal/P-07/2013. KG acknowledges the financial support in the framework of CSR-IC-ICBL-25/CRS-1222014-15/1218 project.

Reference

1. Yoshizava Y, Oguma S, Yamauchi K (1988) New Fe-based soft magnetic alloys composed of ultrafine grain structure. J Appl Phys 64(10): 6044-6046.

2. Herzer G (1990) Grain size dependence of coercivity and permeability in nanocrystalline ferromagnets. IEEE Trans Magn 26(5): 1397-1402.

3. Kane SN, Gercsi Zs, Mazaleyrat F, Varga LK, Coisson M, et al. (2008) Influence of composition and thermal treatments on structural, magnetic and magnetotransport properties of $(Fe_{100-x}Co_x)_{78}Si_9Nb_3B_9Cu_1$ alloys. J Korean Phys Soc 53(96): 3634-3639.

4. Makino A, Kubota T, Yubuta K, Inoue A, Urata A, et al. (2011) Low core losses and magnetic properties of $Fe_{85-86}Si_{1-2}B_8P_4Cu_1$ nanocrystalline alloy with high B for power applications. J Appl Phys 109(7): 07A302–07A302-5.

5. Kane SN, Singh K, Ghodke N, Gupta A, Varga LK (2012) On the optimization of soft magnetic properties of high Bs $Fe_{83.7}B_{14.8}Cu_{1.5}$ nanocrystalline alloy; In: Proc. International Conference on Recent Trends in Physics (ICRTP) J Phys: Conf Series 365(1): 012015/1-4.

6. Wang AD, Men H, Shen BL, Xie GQ, Makino A, et al. (2011) Effect of p on crystallization behavior and soft-magnetic properties of $Fe_{83.3}Si_4Cu_{0.7}B_{12-x}P_x$ nanocrystalline soft-magnetic alloys. Thin Solid Films 519(23): 8283– 8286.

7. Herzer G (2005) Anisotropies in soft magnetic nanocrystalline alloys. J Magn Magn Mater 294(2): 99-106.

8. (2002) International centre of diffraction data PDF-2 database, USA.

9. McHenry ME, Willard MA, Laughlin DE (1999) Amorphous and nanocrystaliine materials for applications as soft magnets Prog. Mater Sci 44(4): 291-433.

10. Varga LK, Bakos E, Kisdi Koszo E, Zsoldos E, Kiss LF (1994) Time and temperature dependence of nanocrystalline structure formation in a Finemet-type amorphous alloy. J Magn Magn Mater 133(1-3): 280-282.

11. Bertotti G (1998) Hysteresis in Magnetism: for Physicists Material Scientists and Engineers (1st edn) New York: Academic Press Inc San Diego, California, USA.

12. Kane SN, Coisson M, Tiberto P, Vinai F, Mazaleyrat F (2011) On the influence of Joule heating induced nanocrystallization on structural and magnetic properties of $Co_{64}Fe_{21}B_{15}$ **alloy**. Current Applied Physics 11: 981-985.

How to cite this article: K Gehlot,S S Modak,L K Varga,S N Kane.Time Dependent Microstructural and Magnetic Properties of Nanocrystalline $Fe_{67.6}Co_{16.9}Nb_5B_{8.5}P_2$ Metallic Alloy. JOJ Mater Sci. 2018; 4(2): 555635. DOI: 10.19080/JOJMS.2018.04.555635

DOI: 10.19080/JOJMS.2018.04.555635

How to cite this article: K Gehlot,S S Modak,L K Varga,S N Kane.Time Dependent Microstructural and Magnetic Properties of Nanocrystalline $Fe_{67.6}Co_{16.9}Nb_5B_{8.5}P_2$ Metallic Alloy. JOJ Mater Sci. 2018; 4(2): 555635. DOI: 10.19080/JOJMS.2018.04.555635